MODELING HIGH FLEXIBLE CLOTHES BASED ON BURSTING TEST RESULTS

L.M. Vas[1], P. Tamás[2], M. Halász[1], A. Décsei-Paróczi[2]
Budapest University of Technology and Economics, Faculty of Mechanical Engineering,
[1] Department of Polymer Engineering
[2] Department of Mechatronics, Optics and Mechanical Engineering Informatics
H-1111 Budapest, Műegyetem rkp. 3., Hungary

ABSTRACT

The bursting test is a simple procedure to study the high deformation of clothes subjected to two-axial loads by a suitable apparatus fastened on a tensile tester. This makes it possible to survey the fabric behaviours from little deformations until failure in a way independent of direction.

Results of analysing the properties of the ball deformed shape of sheet samples and those of measurements obtained by quasi-static tensile tests and bursting tests as well as by comparing them are presented.

1. INTRODUCTION

On modelling common behaviour of human clothes or technical textiles one will face some difficulties. Fibrous structures of high elasticity such as knitted clothes exhibit nonlinear and time-dependent mechanical properties that are to be considered in simulations (Gersak et al., 2013).

Most of the short term and time-dependent mechanical behaviours such as tensile strength properties, creep, stress relaxation and quasi-static hysteresis can be tested on tensile tester. The most general load of textiles is not uniaxial but biaxial that can also be realized by special accessories such as the classical ball burst test in Gyimesi (1968) or ASTM D6797 (2002) as well as that in Al-Gaadi et al. (2010).

We used the bursting test to study the high deformation of the clothes subjected to two-axial loads by a suitable apparatus fastened on a tensile tester. Regarding its execution it is similar to a simple compression test without any sample preparing or gripping problems unlike the tensile test. This makes it possible to survey the fabric behaviours from little deformations until failure in a way independent of direction. The classical evaluation of measurements is based on the assumption that the ball deformed shape of the fabric sample consists of a spherical cap tightened onto the ball and a free surface that can be considered conical as treated in e.g. Gyimesi (1968) and Zhang et al. (2000). Measurements and simulation performed by us earlier showed that in case of large deformability the free surface was not conical but a concave surface as in Halász et al. (2012).

Presentation is on the results of studying and analysing the properties of the ball deformed shape of sheet samples and those of measurements obtained by quasi-static tensile tests and bursting tests performed on clothes of high elasticity as well as the results of comparing the different types of tests.

2. BURSTING TEST PROCESS

The burst test apparatus applied and attachable to a tensile tester and its classical scheme can be seen in Fig. 1. A sample of thin and flexible fabric or sheet is clamped by the circular gripping frame (its radius is R_0) without tension and a compressional load (F_B) is exerted by a steel ball of radius R causing a bulging of the specimen. The height of bulging is denoted by H while α is the bulging angle. The ball is moved by the crosshead with constant-rate-extension until rupture occurs.
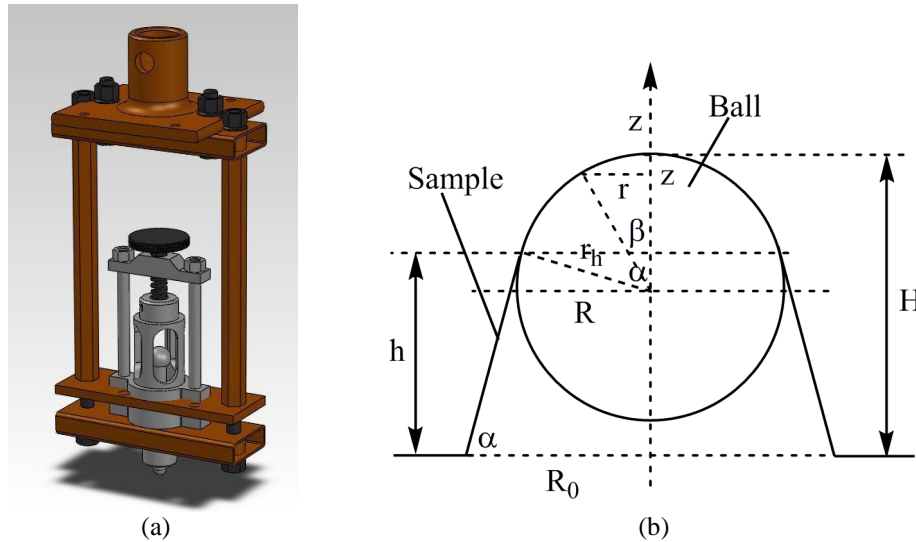

Figure 1: Ball bursting apparatus (a) and the classic scheme of bursting (b)

2.1 Evaluation Based on Conical Approach

In case of isotropic and homogeneous material the deformed shape is a surface of rotation because of the symmetrical arrangement. In general the mechanical behaviour of the sample can be treated with the elastic membrane theory (bending stiffness can be neglected) as applied by Zhang et al. (2000) who obtained the following equations for the meridian (f_1) and hoop (f_2) line stresses (tensile forces related to unit section length instead of cross section) for the spherical cap subjected to axial-symmetric load:

$$\frac{d}{d\beta}(rf_1) - R_1 f_2 \cos\beta + (p_1 - \mu p_r)rR_1 = 0 \tag{1}$$

$$\frac{f_1}{R_1} + \frac{f_2}{R_2} = p_r \tag{2}$$

where r(z), $0 \leq z \leq H$, is the radius function of the generatrix curve in the meridian plane, R_1 and R_2 are the principal curvature radii at a surface point in the meridian and the normal planes respectively, β is the meridian arc angle, while $p_1 = -p\sin\beta$ and $p_r = p\cos\beta$ respectively are the meridian and normal components of the specific external load (p) that is evenly distributed on the spherical cap the resultant of which is the measures force (F_B) (Fig. 1.b):

$$p = \frac{F_B}{2\pi R^2 (1 - \cos\alpha)} \tag{3}$$

Zhang et al. (2000) considered the free surface conical as well, for which p=0, however they took the friction effects between the sample and ball into account as well with the friction coefficient μ. Accordingly, on the basis of Equations (1) and (2) they found that line stresses on the spherical cap are as follows (0≤β(z)≤α; h≤z≤H; β=arccos(z/R)):

$$f_1 = \frac{F_B}{2\pi R(1 - \cos\alpha)}\left(\frac{1}{1 + \cos\beta} + \mu\frac{\sin\beta}{3}\right) \tag{4}$$

$$f_2 = \frac{F_B}{2\pi R(1 - \cos\alpha)}\left(\cos\beta - \frac{1}{1 + \cos\beta} - \mu\frac{\sin\beta}{3}\right) \tag{5}$$

The meridian line stress in the conical section ($R_1 = \infty \Rightarrow f_2 = 0$) is given by:

$$f_1 = \frac{F_B}{2\pi r(z)\sin\beta}, \qquad r(z) = R_0 - \frac{R_0 - R}{h}z \tag{6}$$

2.2 Concave Free Surface Observed and Simulated

According to our measurements when the deformability is large as it is in Fig. 2.a (knitted lining net lace material, area density: 101 g/m^2, thickness: 0.27 mm) then the free surface is observably not a truncated cone but a concave one.
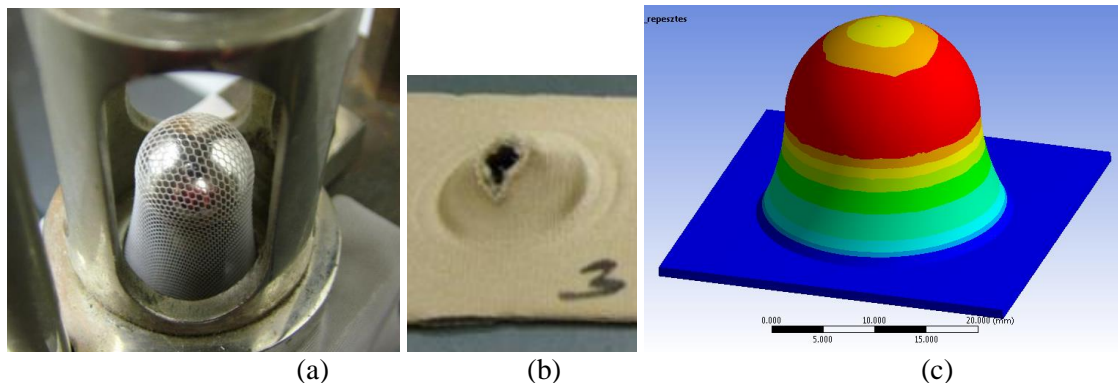

(a)   (b)   (c)

Figure 2: Concave deformed shape of material of large deformability (a) as well as shape of rupture (b) and stress results of FEM simulation performed for foam laminated knitted fabric (c)

Based on measurements on foam laminated 3 layer knitted fabric (area density: 440 g/m^2, thickness: 2.57 mm) this phenomenon was simulated by a FEM model (Ansys) in Halász et al. (2012) using hyperelastic material of Mooney-Rivlin type (Fig. 2.c). In addition results of simulation showed that the stress on the spherical cap is larger than that on the free surface and the maximum stress values can be found on the lower part of the spherical section (Fig. 2.c). This is confirmed by some observations that the first breakage of yarns took place not on the ball top but lower (Fig. 3.a) therefore the split at rupture (Figs. 2.b. and 3.b) cannot be found in the middle.

(a)   (b)

Figure 3: Beginning of the rupture of a knitted lining material (area density: 153 g/m^2, thickness: 0.42 mm) (a) and the shape and position of the split (b)

2.3 Analysis Based on Catenary Approach

It can be supposed that a free surface wants to take on a shape belonging to minimum strain energy that is concave according to Fig. 2.a hence it is inside of the truncated cone and the generatrix runs below the tangent of the sphere (Fig. 4). In case of isotropic homogeneous and elastic membranes this can be reached by an area minimum. It is known that the minimal surface of rotation between two circular frames that minimizes its area is a catenoid made by rotating a catenary (chain curve) around the axis as it is in H. Pálfalvi (2002) and Hegedűs (2015). This is a membrane surface the generatrix of which is given by a two free parameter (c_1, c_2) function ($c_0 = 1$) and the first two boundary conditions below:

$$r(z) = \frac{c_0}{c_1}\cosh(c_1 z - c_2) \qquad r(z) = \begin{cases} R_0, & z = 0 \\ r_h, & z = z_h \end{cases} \qquad r'(z) = r'_h, \quad z = z_h \tag{7}$$

When fixing the two end of the minimum surface other constraint cannot be satisfied hence the tangents are not equal to each other at the boundary (Fig. 4).
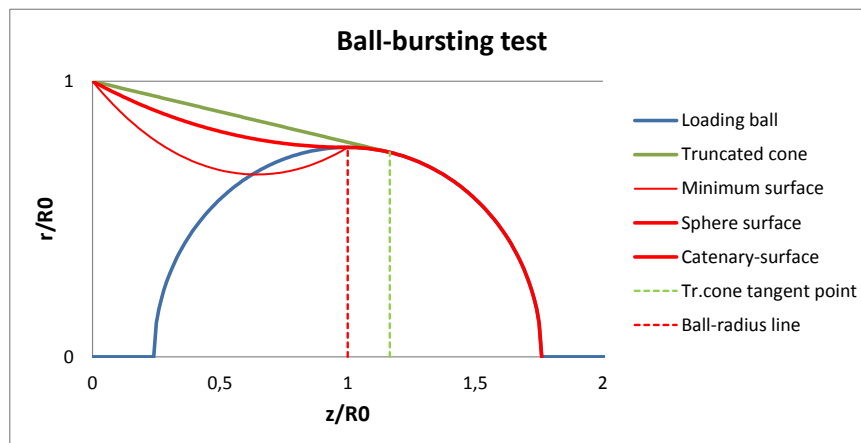

Figure 4: Schematic normalized plane section of the middle surface of the deformed specimen along the axis of rotation (H/R_0=1.76) in cases of different approaches (min. surf: c_0=1, c_2=$c_1 R_0$=1.316; catenary: c_0=0.589, c_2=$c_1 R_0$=0.775)

Completing the function by Equation (7) with an additional free parameter, c_0, this third boundary condition in Equation (7) can also be satisfied. Equation (7) with 3 free

parameters describes a catenary that is its generatrix is a chain curve however its area is not minimal. According to observations the tangent at the boundary is approximately zero (Fig. 2) therefore the catenary (chain) curve in Fig. 4 realizes this case for which the generatrix curve meeting the boundary conditions by Equation (7) is as follows ($0 \leq z \leq h = H-R$, $H>R$):

$$r(z) = R\cosh\left(\left(\frac{z}{H-R}-1\right)a\cosh\left(\frac{R_0}{R}\right)\right) \tag{8}$$

Fig. 5 shows the linear and area deformations of the sample respectively calculated from the meridian length and total area of the deformed surface. It can be seen that the catenary surface provides about the same linear strain − 2-4% larger at small bulging − but smaller area strain than that by the truncated cone. For the latter the difference increases with bulging height (H) and its maximum value at $z=5R$ is about 0.29 (29%). It is not small however relating that to the total area strain gives less than 5%.
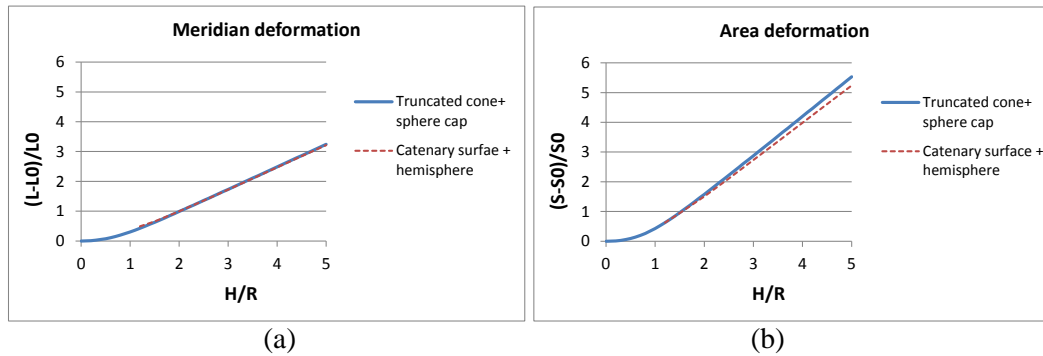

<table>
<tr><td>(a)</td><td>(b)</td></tr>
</table>

Figure 5: Linear meridian (a) and area (b) strain as a function of the normalized bulging

For the catenary surface by Equation (8) $R_2<0$ is valid and the line stresses and the parameters are given by:

$$f_1(z) = \frac{F_B}{2\pi}\frac{\sqrt{1+r'^2(z)}}{r(z)} = \frac{F_B}{2\pi}\frac{c_1\sqrt{1+c_0^2\sinh^2(c_1z-c_2)}}{c_0\cosh(c_1z-c_2)} \tag{9}$$

$$f_2(z) = -f_1\frac{R_2}{R_1} = \frac{F_B}{2\pi}\frac{c_0c_1\cosh(c_1z-c_2)}{\sqrt{1+c_0^2\sinh^2(c_1z-c_2)}} \tag{10}$$

$$c_0 = c_1R; \quad c_1 = \frac{c_2}{H-R}; \quad c_2 = a\cosh\left(\frac{R_0}{R}\right) \tag{11}$$

In Fig. 6 the variation of the meridian line stress normalized by $f_0=F_B/2\pi R_0$ is depicted for the classical truncated cone and the catenary as free surface according to Equations (6) and (9) respectively. The meridian stress on the spherical cap was calculated with Equation (4) at different friction coefficients supposing that it is not larger than that (f_1^*) obtainable in case of a spherical free surface (dashed red curve in Fig. 6) ($0<\beta\leq\alpha$):

$$f_1^* = \frac{F_B}{2\pi R \sin^2 \beta}$$
(12)

According to the calculations the catenary surface gives larger meridian stresses than the conical one (Fig. 6.a: I) however the maximum stress arises at the upper boundary (μ=0) or in its vicinity (μ>0) (Fig. 6.a: II).
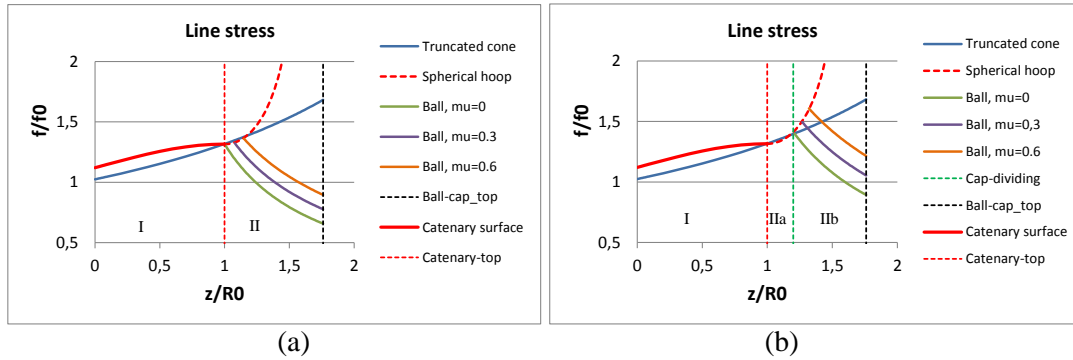

(a)   (b)

Figure 6: Normalized meridian stress along the axial section of the deformed sample without (a) and with (b) free hoop (IIa) on the spherical cap (mu=μ)

Vertical red and green dashed lines respectively indicate the external boundary of the spherical cap (Fig. 6.a: II) and an internal separating one above which the material resistance generated pressure, p, arises and effective (Fig. 6.b: IIb). Below the latter a free hoop on the ball (Fig. 6.b: IIa) behaves like a free spherical segment where pressure does not arise. Hence this increases the pressure according to Equation (3). Fig. 6.b illustrates the variation of the meridian stress under these conditions. This effective cap reduction causes a stress peak on the remaining part that increases with the friction coefficient (Fig. 6.b). This situation may give a possible explanation for the place of rupture as shown in Fig. 3.

3. EXPERIMENTAL PROCEDURES

3.1. Test material

The material tested was a plain weave fabric made of special false twisted multifilament PET yarns (Table 1).

Table 1. Nominal data of the fabric and its yarns

Yarn			Fabric		
Material	**Linear density** [dtex]		**Type of weave**	**Yarn density** [1/100 mm]	**Area density** [g/m^2]
PET	warp	weft	plain	warp	weft	177
	333			252	240	

3.2. Tensile tests

In order to provide proper basis for analysis tensile tests were carried out on yarns of 50 mm gauge length as well as on fabric samples of 50 mm width and 100 mm length cut

out in directions 0 (warp), 15, 30, 45, 60, 75, and 90 (weft) degrees earlier as found in Vas et al. (2013). The instrument applied was a Zwick Z020 universal tensile tester. In every case the rate of elongation was 100 mm/min and the number of measurements was 3. Results of tensile tests are summarized in Tables 2 and 3 and depicted in Figs. 7 where the values of the breaking force are related to the width of the samples. For the sake of comparison blue line zones show the yarn strength limits (10.8-12.7 N/yarn, 26.8-34.5 %) related to the number of yarns in 1 mm width in case of the breaking force.

Table 2. Breaking force results of tensile test of fabric specimens cut out different directions

Spec. breaking force	Cutting angle [deg]						
[N/mm]	**0**	**15**	**30**	**45**	**60**	**75**	**90**
Minimum	26,0	9,5	9,4	14,6	6,9	6,9	22,1
Maximum	27,0	10,4	11,9	15,4	7,4	7,9	23,1
Mean	26,5	10,1	10,9	15,0	7,2	7,3	22,7
Standard deviation	0,72	0,45	1,32	0,40	0,28	0,57	0,55
Coeff. of variation [%]	2,72	4,50	12,17	2,67	3,82	7,78	2,41

Table 3. Breaking strain results of tensile test of fabric specimens cut out different directions

Breaking strain	Cutting angle [deg]						
[%]	**0**	**15**	**30**	**45**	**60**	**75**	**90**
Minimum	30,8	23,2	31,5	40,9	28,5	18,5	22,5
Maximum	30,9	24,7	35,9	45,5	30,5	19,1	23,9
Mean	30,9	24,0	34,1	43,4	29,8	18,7	23,1
Standard deviation	0,05	0,76	2,30	2,33	1,10	0,36	0,72
Coeff. of variation [%]	0,16	3,16	6,74	5,37	3,69	1,93	3,14

According to the results the tensile strength properties strongly depend on the cutting angle. Two local minimums and a maximum can be found in directions 15°, 75°, and 45°, respectively concerning both the breaking force and the strain (Figs. 2 and 3). On the other hand the tensile strength rapidly decreases on going from the main directions (warp: 0°, weft: 90°) to 45° as well as the global maximum of the breaking force can be found in warp direction while the breaking strain shows that in the 45° direction. The strength of fabric is smaller than that of yarns which can be attributed to the crimping, while the yarn breaking strain forms a kind of mean among the fabric ones.
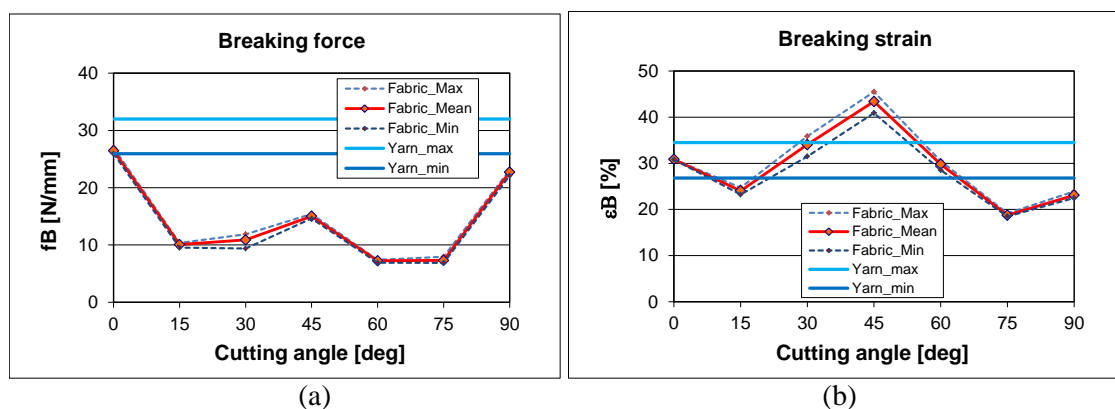

Figure 7: Measured values of the specific tensile breaking force (a) and the breaking strain (b) versus cutting angle

3.3. Ball-bursting tests

For the ball burst apparatus used (Fig. 1.a) the radii of the ball and the clamping frame were R=9.5 mm and R_0=12.5 mm respectively, the maximum height of bulging was H_{max}=45 mm, while the extension rate was set at v=100 mm/min. The measuring process of one of the 4 samples tested and the shape of the burst splits can be seen in Fig. 8.
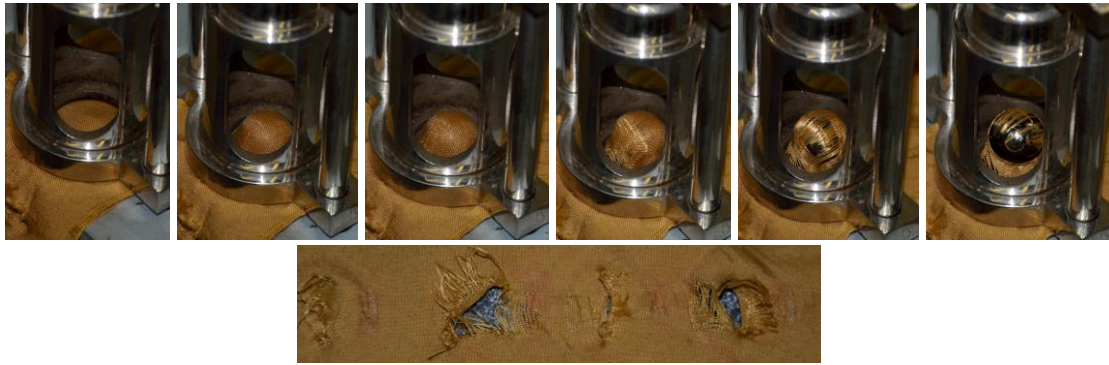

Figure 8: Deformation process of the woven fabric sample during the ball burst test and the shape of the split holes

Recorded burst force versus bulging relationships and their point by point average are shown by Fig. 9 while the strength properties belonging to the first and the maximum force peaks are contained by Table 2.

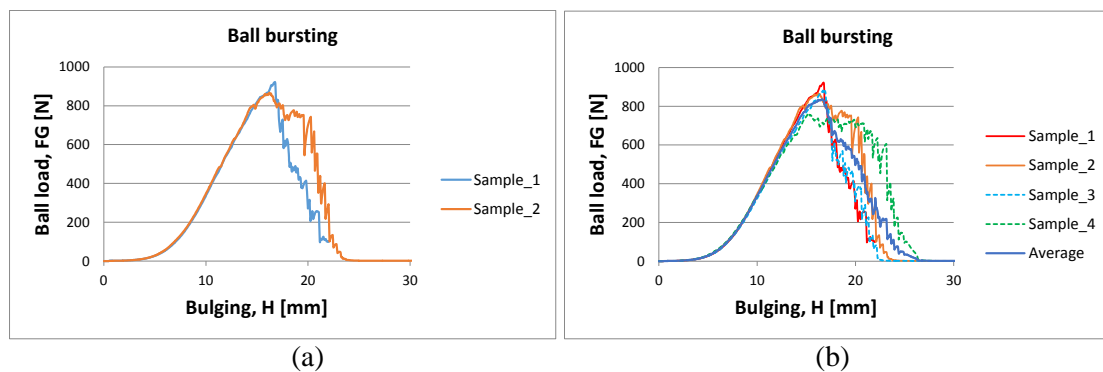(a)   (b)

Figure 9: Typical load-deformation relationships (a) and the average of four measurements (b)

Table 4. Numerical strength results of ball bursting tests

Properties	S_1	S_2	S_3	S_4	S_av	Minimum	Maximum	Mean	SD	CV [%]
F_peak1 [N]	813,8	792,7	881,8	764,3	804,0	764,3	881,8	813,2	50,1	6,2
H(F_peak1) [mm]	15,2	14,4	16,7	15,3	15,2	14,4	16,7	15,4	1,0	6,2
Fmax [N]	922,5	867,1	881,8	764,3	835,2	764,3	922,5	858,9	67,3	7,8
H(Fmax) [mm]	16,8	16,2	16,7	15,3	16,6	15,3	16,8	16,2	0,7	4,3

4. DISCUSSION

For the sake of comparing the strength properties obtained by tensile and burst tests the measured breaking or bursting force values were related to the sample width or the cross section circumferences providing line stress values as they are in Tables 2 and 5.

Table 5. Line strength and meridian strain results of ball bursting tests

Properties	Minimum	Maximum	Mean
f_peak1 [N/mm]	12,8	14,8	13,6
ε (f_peak1) [mm]	64,0	81,2	71,4
fmax [N/mm]	12,8	15,5	14,4
ε (fmax) [mm]	70,7	82,0	77,4

In Fig. 10.a shows the tensile strength of the fabric as a function of the cutting angle like in Fig. 7.a completing with minimum and maximum values of the bursting strength indicating by the horizontal straight lines.
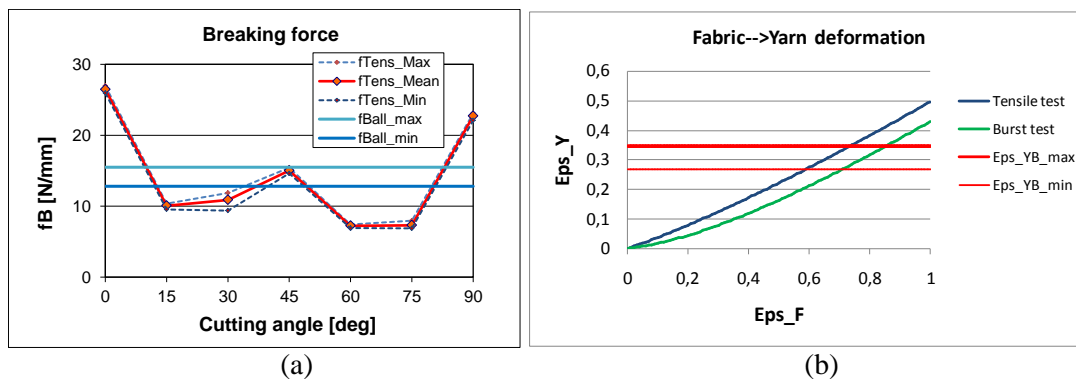

(a)   (b)

Figure 10: Specific breaking force versus cutting angle (a) and the relationship between the strains of the fabric and its yarns (b) in cases of tensile and burst tests

According to the measurements the bursting strength calculated as an average along the cross section of the deformed sample seems to be a kind of "mean" of the tensile strength values measured in different directions indicating that the stress distribution in the cross section of the bulged biaxial sample is not uniform. This is confirmed by the fact that the damage in sample is caused by yarn breakage and the observations that during the extension-controlled burst test the first damage was realized by the breakage of the weft yarns having smaller breaking strain.

The deformations of the fabric samples were measured during the tests however these are just the projection of the crimped yarns. Hence the differences in tensile strain (Table 3) and meridian burst strain (Table 5) may be attributed to the different changes of the yarn crimping. This can be supported by calculating the yarn strain as a function of the fabric strain taking into consideration a yarn crimping of 50% and different rates of crimping reduction for the tensile (nu=0.1) and burst (nu=0.5) tests. In Fig. 10.b the red zone shows the minimum and maximum values of the yarn breaking strains (26.8-34.5%) measured earlier in Vas et al. (2013). The projections of the intersection points of the zone limits and the calculated yarn strain curves are the proper fabric strain limits. This zone for the burst test (71-86%) essentially covers the strain range belonging to the maximum force in Table 5. The zone for the tensile test (59-74%) is much higher than the values in Table 3 or Fig. 7.b. The deviation may be explained by the larger bending load caused by the larger yarn crimping at breakage. On the other hand the biaxial and shearing deformations of the bulged sample can increase the extensibility of the fabric relating to the uniaxial test where the crosswise yarns increase the bending load the lengthwise yarns by strong contraction. This is confirmed by the fact that about H=10

mm bulging an inflexion point can be identified on all the records (Fig. 9) which belongs to circ. 33% meridian strain being about the tensile strains in main directions (Fig. 7.b). Of course these deformation phenomena need further examinations.

5. CONCLUSIONS

On the basis of the theoretical and experimental analysis of the ball burst test it can be stated that to a usual evaluation the truncated cone as a free surface can be applied with relatively small error (<5% for both linear and area strain) in case of large elasticity textiles however more precious examinations of textiles need the catenary approach and the revelation of the yarn deformation circumstances and/or FEM simulation with taking into account the biaxial structure. All these can give base for estimating the tensile strength properties from the much simpler ball burst test.

5. REFERENCES

Gersak J. (edited by), Halász M., Tamás P., Kokas-Palicska L., "Complex Fabric Deformations and Clothing Modelling in 3D," Lambert Academic Publishing, Saarbrücken, 2013.

Al-Gaadi B., Molnár K., Halász M., Vas L.M., Tamás P., Molnár J., Hegyi D., "Biaxial mechanical testing method using image processing," In: Aachen Dresden International Textile Conference, Dresden, Germany, 25-26. Nov. 2010., 121-125 (2010).

Gyimesi J., "Physical Testing of Textile Materials", (in Hungarian), Műszaki Könyvkiadó, Budapest, 774-776, 1968.

ASTM D 6797 – 02: "Standard Test Method for Bursting Strength of Fabrics Constant-Rate-of-Extension (CRE) Ball Burst Test1," 2002.

Zhang X., Li Y., Yeung K.W., Miao M.H., and Yao M., "Fabric-bagging: Stress Distribution in Isotropic an Anisotropic Fabrics," Journal of the Textile Institute, 91 Part I. No. 4, 563-576, 2000.

Halász M., Décsei-Paróczi A., Tamás P., Vas L.M., "Modeling High Flexible Underclothes Based On Bursting Test Results," In: Borbély Á. Eds., 3rd International Joint Conference on Environmental and Light Industry Technologies: International Symposium on Innovative Technologies and Design, Óbuda University Budapest, Hungary, 21-22. Nov. 2012., Proceedings CD p. (2012).

Hegedűs I., "3. Momentless load bearing of shells: the membrane theory," (in Hungarian) Budapest University of Technology and Economics, Department of Bridges and Constructions, www.hsz.bme.hu/hsz/dolgozok/feltoltesek/ihegedus/hejuj2.doc

H. Pálfalvi D., Hegedűs I., "On The Multiple Solution Of Axisymmetric Minimum Surfaces," Journal of Computational and Applied Mechanics, 3(2) 157-167, 2002.

Vas L.M., Göktepe F., Péter P., Marianna M., Özdemir D., Kokasné-Palicska L., Szakály N., "Modeling and Analysing the Tensile Behavior of Fabric Samples," Acta Polytechnica Hungarica, 10(3), 79-95, 2013.

ACKNOWLEDGEMENTS